

SEISMIC BEARING CAPACITY WITH VARIABLE SHEAR TRANSFER

X Shi¹, and R. Richards, Jr²

ABSTRACT

The seismic degradation of bearing capacity for drained soils is shown to depend primarily on two factors related to earthquake acceleration: (a) the lateral inertial forces in the structure transmitted as shear at the foundation-soil interface and (b) the lateral body forces in the soil itself. Both induce shear stresses using up the reserve strength of the soil to carry the footing load. During those short periods when this reserve strength provided by the static design factor of safety is exhausted, the footing settles and moves laterally. Solutions for this seismic limit state defining the critical acceleration at which it occurs are determined for any value of shear transfer first by the "exact" method of characteristics and then by a simple Coulomb-type approximate mechanism. Expressions for seismic bearing capacity factors that are directly related to their static counterparts are nearly identical by either method. Thus a straightforward sliding block procedure based on the Coulomb mechanism with examples is presented for computing accumulating settlements due to the periodic loss of bearing capacity. Conversely, this approach leads to a modified static design procedure for shallow footings to limit seismic settlements in a prescribed earthquake intensity zone.

INTRODUCTION

Seismic settlement of foundations due to periodic bearing capacity reduction rather than densification or liquefaction was first explained in a general way by fluidisation theory for the half-space [Richards et al, 1990a]. As the first application of this free-field solution, the seismic bearing capacity using the Prandtl mechanism was presented by Richards et al [1990b]. Other recent research [Richards et al, 1993; Richards and Shi, 1991; and Sarma and Iossifelis, 1990] attempts to quantify this behaviour for the case where it is assumed that the shear induced by the inertial force of the supported mass is fully transferred by the footing to the supporting soil. Further, the approach using the Prandtl-type mechanism has been modified by Budhu and Al-Karni [1993] to derive a similar but different expression for seismic bearing capacity factors including the effect of vertical acceleration. Their approach is somewhat empirical and applies also only for full shear transfer.

In many cases when isolated footings are used, the shear transfer may be reduced or magnified by the design of the superstructure. An example of a two-span bridge on a central pier is shown in Figure 1 where, for simplicity, the relative stiffness of the pier is assumed negligible eliminating moment transfer to the footing and the possibility of rocking. Thus, for this example, the shear transfer coefficient, "f", defined as the fraction of the vertical footing load times the horizontal

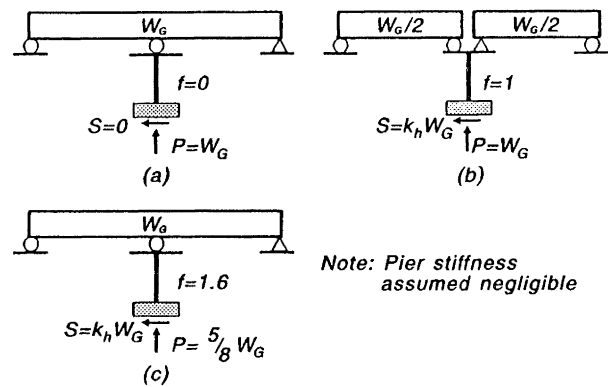


FIGURE 1 Variation of shear transfer for different bridge constructions $S = f k_h P$, where k_h = horizontal acceleration coefficient

acceleration coefficient k_h (ie, $k_h P$) transferred as shear force, S , varies from 0 to 1.6 depending on the support condition of the girder.

For this paper, two methods of limit analysis are used to calculate the seismic bearing capacity of strip footings with variable shear transfer:

1. the method of characteristics;
2. limit equilibrium, using a Coulomb mechanism with sliding active and passive wedges.

¹ Bridge Engineer, Frederic R. Harris Inc., New York, NY 10017, USA

² Professor, Dept. of Civil Engineering, SUNY at Buffalo, Buffalo, NY 14260, USA

The results of each method are compared to each other and to those obtained by Sarma and Iossifelis [1990]. Since the agreement is so close, only the Coulomb Mechanism is presented in any detail. Moreover, this approximate mechanism leads to simple calculations of seismic settlement by the sliding block method proposed by Newmark [1965] for slopes and used by Richards and Elms [1979] for retaining walls. Thus a straightforward design approach is possible to either eliminate seismic settlements due to loss of bearing capacity or limit them to an acceptable level. It is assumed throughout that the foundation soil is drained and the shear strength is a constant given by the cohesion and friction angle.

SOLUTION BY THE METHOD OF CHARACTERISTICS

The method of characteristics to compute static bearing capacity was developed in detail by Sokolovsky [1960]. In general this approach can be extended to the seismic situation with the only modification being the introduction of horizontal and vertical body forces $k_h\gamma$ and $k_v\gamma$ as shown in Figure 2 where other terms are also defined. The general field equations for horizontal and vertical equilibrium are:

$$\frac{\partial \sigma_x}{\partial x} + \frac{\partial \tau_{zx}}{\partial z} = -k_h\gamma$$

$$\frac{\partial \tau_{xz}}{\partial x} + \frac{\partial \sigma_z}{\partial z} = (1 - k_v)\gamma \tag{1}$$

The introduction of a crucial function first proposed by Sokolovsky [1960]

$$x = \frac{1}{2} \cot \phi \ln \frac{\sigma}{c} \tag{2}$$

for a Mohr-Coulomb material leads to a solution procedure by finite differences for the resulting hyperbolic equations. These equations are complicated particularly in the transformed domain where a shooting technique is used to solve them. Complete details of the procedure with inertial body forces is given by Shi [1993] which follows that given by Harr [1966] for the static case. Only the results for the seismic case are presented and discussed in this paper.

The seismic bearing capacity p_{LE} can be written as:

$$p_{LE} = cN_{cE} + qN_{qE} + \frac{1}{2} \gamma BN_{\gamma E} \tag{3}$$

corresponding to its static counterpart:

$$p_{LS} = cN_{cS} + qN_{qS} + \frac{1}{2} \gamma BN_{\gamma S} \tag{4}$$

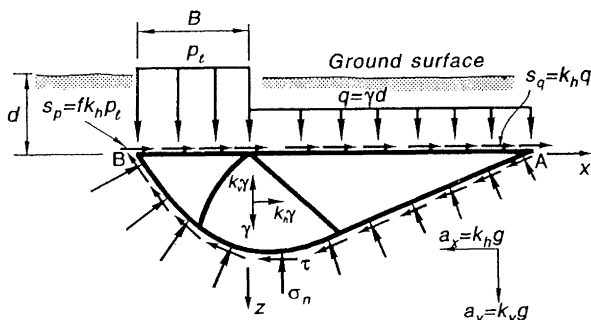


FIGURE 2 Stresses on the failure surface

In these equations the dimensionless coefficients N_c , N_q and N_γ , called bearing capacity factors, represent the contributions of the cohesion, c , surcharge, $q = \gamma d$, and unit weight, γ , to the ultimate limit load intensity p_L for the footing. Throughout, B is the width of the strip footing and the subscript S or E , sometimes lowercase, differentiates between the static or earthquake situation.

While the total bearing capacity can be obtained directly by the method of characteristics for a given set of parameters γ , q , c , ϕ , B , f , and k_h , it gives a clearer picture physically to separate the result into these bearing capacity factors which are then functions of only the friction angle ϕ , the shear-transfer fraction, f , and the horizontal acceleration coefficient, k_h , all of which are also dimensionless. The resulting curves are therefore easy to plot and very powerful for design. For convenience, k_v is neglected but is easily included by multiplying p , q and p by $(1 - k_v)$ throughout.

To determine the individual bearing capacity factors from the method of characteristics, superposition is used from special cases. First N_{qE} is determined when $c = \gamma = 0$. Then p_{LE} is found for only $c = 0$ which gives $\frac{1}{2}\gamma BN_{\gamma E}$ by subtracting qN_{qE} . Finally the general case is computed which gives cN_c by subtracting the previous result. Sokolovsky has demonstrated that results based on this superposition procedure are conservative.

Setting $c = \gamma = 0$, N_{qE} can be determined in closed form as:

$$N_{qE} = \frac{\sin \Delta_1 \sin(\Delta_2 + \delta_2)}{\sin \Delta_2 \sin(\Delta_1 - \delta_1)} \exp\left[(\pi - \Delta_1 + \delta_1 - \Delta_2 - \delta_2) \tan \phi\right] \tag{5}$$

which is the same as the classic formula for inclined loading [Harr, 1966]. In the dynamic case however, the delta factors in Equation 5 include k_h and are given by:

$$\delta_1 = \tan^{-1} \left[\frac{k_h q(x)}{q(x) + c \cot \phi} \right]; \quad \delta_2 = \tan^{-1} \left[\frac{k_h f p(x)}{p(x) + c \cot \phi} \right];$$

$$\Delta_1 = \sin^{-1} \left[\frac{\sin \delta_1}{\sin \phi} \right] \quad \text{and} \quad \Delta_2 = \sin^{-1} \left[\frac{\sin \delta_2}{\sin \phi} \right] \tag{6}$$

Figure 3a shows the ratio of N_{qE} to $N_{qS} = 18.4$ for $\phi = 30^\circ$ for three values of shear transfer where, as shown in Figure 2, the shear stress at the base of the footing is $s_p = f k_h p$.

Following our superposition procedure, the parameter γ is now introduced, p_{LE} determined, and qN_{qE} from Equation 5 subtracted to determine $N_{\gamma E}$. At this point let us introduce the dimensionless variables $B' = B/\ell$, $q' = q/\gamma\ell$, $p' = p/\gamma\ell$, $c' = c/\gamma\ell$ where ℓ is a characteristic length (usually B). Also we should note that an interesting difficulty now arises in the method of characteristics due to the governing equation being of a hyperbolic type [Harr, 1966]. For a solution to exist, we cannot specify the contact stresses over the entire boundary and either $q(x)$ or $p(x)$ must be left as an unknown in addition to the shape of the failure surface. Thus, although we would like to determine the value of a constant limit load intensity p_L and $s = f k_h p_L$, this is not possible since q is specified as constant on boundary OA in Figure 2. To illustrate, the actual distribution of p_L along $B' = 1$ is plotted in Figure 4 for the static case $k_h = 0$ and three values of q' . Thus by the method of characteristics there is actually a small moment due to the eccentricity of the total limit load $P_L = \int p_L dx$ which helps the failure surface develop somewhat sooner than would be the case

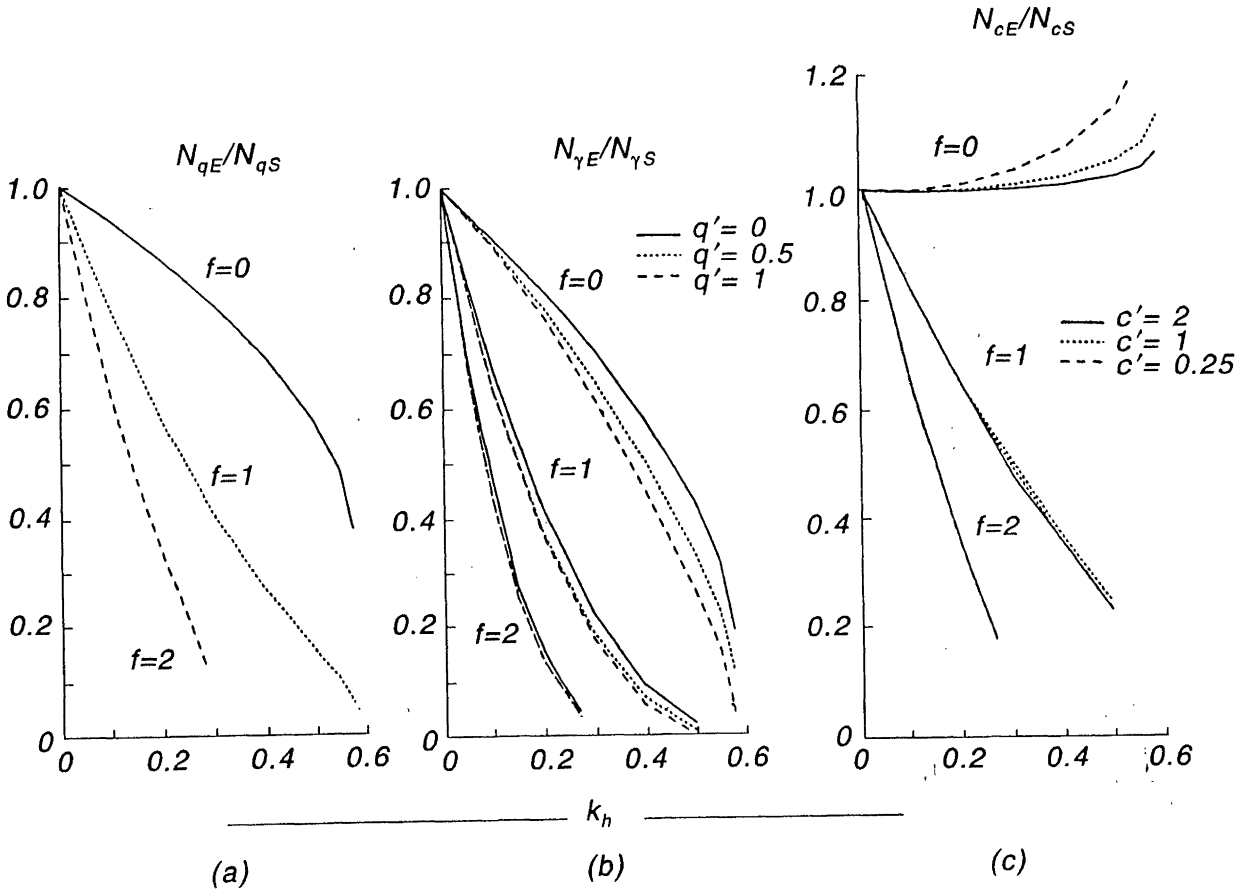


FIGURE 3 Comparison of the ratio of seismic to static coefficients for $\phi = 30^\circ$ (Characteristics)

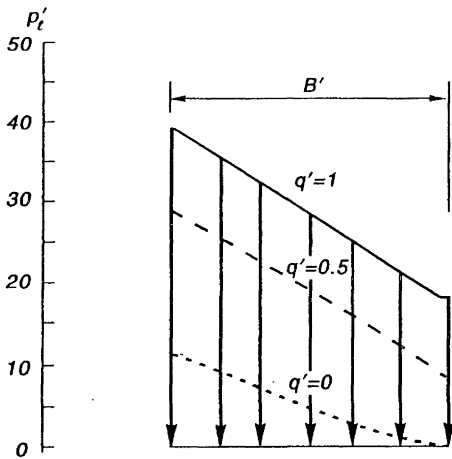


FIGURE 4 Dimensionless loading distributions for $\phi = 30^\circ$, $c = 0$, $\gamma > 0$ and $k_h = 0$ (static case)

if p_L were actually constant. This moment from the method of characteristics is always neglected and $p_L = P_L/B$ is considered uniform in calculating the bearing capacity factors.

The ratio of $N_{\gamma E}$ to $N_{\gamma S}$ for $\phi = 30^\circ$ is plotted in Figure 3b for three values of f and three different q' values. As was true for N_{qE} , the bearing capacity due to γ decreases rapidly with the severity of the earthquake acceleration. Equally dramatic is the pronounced effect of shear transfer. However $N_{\gamma E}$ is relatively insensitive to q' and the value of $q' = 0.5$ will be used to

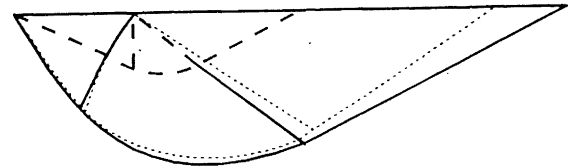


FIGURE 5 Comparison of slip surfaces for $\phi = 30^\circ$, $c = 1$ and $q = 0.5$; (a) $k_h = 0.4$ with $f = 0$ (solid), (b) the static case where $k_h = 0$ (dotted) and (c) $k_h = 0.4$ with $f = 1$ (dashed)

determine N_{cE} in the third step of the superposition procedure. To calculate N_{cE} the cohesion, c , is considered as a variable not equal to zero (q and γ constant). As an example, the ratio of N_{cE} to N_{cS} as a function of k_h for $q' = 0.5$, $\phi = 30^\circ$ and three values of c' is plotted in Figure 3c. The increase in N_{cE} with increasing k_h for $f = 0$ can be explained by the slip surfaces shown in Figure 5. The dotted line is the static failure surface. Since the solid line which represents the seismic surface at $k_h = 0.4$ for $f = 0$ is actually longer, the resistance due to cohesion c is larger. Thus, while the total bearing capacity decreases the portion due to c increases slightly for base-isolated footings. For comparison, the dashed line shows the slip surface for a fully bonded footing. Similar to changing q' in the previous case, changing c' has little effect on the N_{cE} to N_{cS} ratio and the interdependence between c' and q' is insignificant. This insensitivity to changes in q' and c' has been verified for $10^\circ \leq \phi \leq 40^\circ$. Thus, using rounded values of $c' = 1$ and $q' = 0.5$ is justified for design.

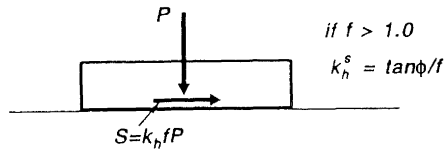


FIGURE 6 Base sliding mechanism

It must be pointed out that for a shear transfer ratio $f \leq 1$, the curves in Figure 3 of the ratio of N_{qe}/N_{qs} and $N_{\gamma e}/N_{\gamma s}$ for cohesionless soil end at the cut-off acceleration $k_h = \tan \phi$ because the soil becomes generally fluidized [Richards et al., 1900a]. For $f > 1$ at high accelerations, a base sliding mechanism as shown in Figure 6 instead of a bearing capacity failure occurs at $k_h^s = (\tan \phi) / f$ and the curves must end at this transition.

BEARING CAPACITY BY THE COULOMB MECHANISM

Richards et. al [1993] and Richards and Shi [1991] present a simple Coulomb mechanism to obtain the approximate seismic bearing capacity with full shear transfer, $f = 1$. Also in this earlier work the cohesive bearing capacity factor N_{ce} was only presented as an empirical approximation. Here the Coulomb mechanism is extended to allow any value of f and the cohesive contribution to strength is also derived from fundamental force equilibrium requirements.

First, consider a cohesionless soil. For the free body diagram shown in Figure 7, equilibrium of horizontal and vertical forces for the active wedge requires that:

$$R_A \sin(\rho_A - \phi) + k_h W_A + S_{PE} = P_{AE} \cos \delta \quad (7)$$

and

$$W_A + P_{LE} = R_A \cos(\rho_A - \phi) + P_{AE} \sin \delta \quad (8)$$

Substituting Equation (7) and (8) and rearranging with

$$W_A = \frac{1}{2} \gamma H^2 \cot \rho_A, P_{LE} = p_{LE} H \cot \rho_A \text{ and } S_{PE} = f k_h P_{LE} :$$

$$P_{AE} = \left[\frac{2p_{LE}}{H} + \gamma \right] A_1 \frac{H^2}{2} + \left[\frac{2p_{LE}f}{H} + \gamma \right] A_2 \frac{H^2}{2} \quad (9)$$

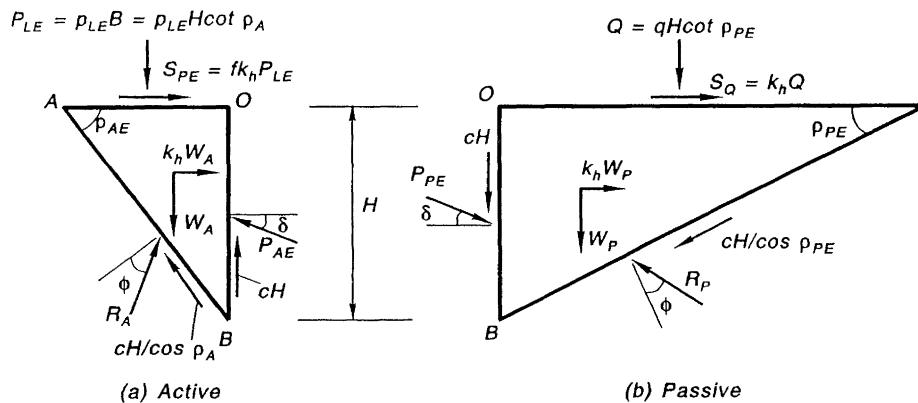


FIGURE 7 Free body diagram of the Coulomb mechanism

where

$$A_1 = \frac{\sin(\rho_A - \phi)}{\cos(\rho_A - \phi - \delta)} \cot \rho_A \quad (10)$$

$$A_2 = \frac{k_h}{\tan(\rho_A - \phi)} A_1 \quad (11)$$

The critical condition occurs when P_{AE} is maximum which depends on ρ_A and the limit load p_{LE} .

Similarly, for the passive wedge the thrust P_{PE} is:

$$P_{PE} = \frac{1}{2} \gamma H^2 K_{PE} + q H K_{PE} \quad (12)$$

where from the M-O equations [Richards and Elms, 1987]:

$$K_{PE} = \frac{\cos^2 \alpha}{\cos \theta \cos(\delta + \theta) \left[1 - \sqrt{\frac{\sin(\phi + \delta) \sin \alpha}{\cos(\delta + \theta)}} \right]^2} \quad (13)$$

$$\text{where } \theta = \arctan \left[\frac{k_h}{1 - k_v} \right] \text{ and } \alpha = \phi - \theta.$$

At failure, P_{AE} must equal the minimum P_{PE} at a known ρ_{PE} given by

$$\rho_{PE} = -\alpha + \arctan(\kappa) \quad (14)$$

$$\text{where } \kappa = \frac{\sqrt{\tan \alpha (\tan \alpha + \cot \alpha) (1 + \tan(\delta + \theta) \cot \alpha)} + \tan \alpha}{1 + \tan(\delta + \theta) (\tan \alpha + \cot \alpha)}$$

and therefore

$$P_{AE} = \left[\frac{2p_{LE}}{H} + \gamma \right] A_1 \frac{H^2}{2} + \left[\frac{2p_{LE}f}{H} + \gamma \right] A_2 \frac{H^2}{2} = P_{PE} \quad (15)$$

However, P_{AE} involves two unknowns: ρ_A and p_{LE} . Through iteration of equation (15) ρ_A and p_{LE} can be determined to maximize P_{AE} . Finally for cohesionless soil, the seismic bearing capacity p_{LE} can be expressed as:

$$p_{LE} = q N_{qe} + \frac{1}{2} \gamma B N_{\gamma e} \quad (16)$$

where

$$N_{qE} = \frac{K_{PE}}{A_1 + fA_2} \quad (17)$$

$$N_{\gamma E} = \frac{K_{PE} - A_1 - A_2}{A_1 + fA_2} \tan \rho_A \quad (18)$$

As demonstrated previously, using a frictional angle $\delta = \phi/2$ between the interface of the two wedges gives N_{qS} and $N_{\gamma S}$ within 10% of the standard static values for $10^\circ \leq \phi \leq 40^\circ$. Therefore, let us try this arbitrary assumption for seismic analysis and see how it compares with analysis by the method of characteristics. Figure 8a and 8b show the ratios of $N_{\gamma E}$ to $N_{\gamma S}$ and N_{qE} to N_{qS} with different f and varied dimensionless surcharge $q'' = \gamma d/\gamma H = d/H$ for $\phi = 30^\circ$ ($N_{qS} = 16.51$ and $N_{\gamma S} = 23.79$). For $f = 1$ the ratios of $N_{\gamma E}$ to $N_{\gamma S}$ and N_{qE} to N_{qS} are the same as those derived previously. These two sets of curves indicate that, like the solution by the method of characteristics, variation of q has negligible effect on the ratio of the seismic to static coefficients.

As a second step, the cohesive strength is now included. Using the free body diagram of Figure 7 equilibrium of the passive wedge gives:

$$S_Q + k_h W_p + P_{PE} \cos \delta = R_p \sin(\rho_{PE} + \phi) + cL_p \cos \rho_{PE} \quad (19)$$

$$W_p + Q + P_{PE} \sin \delta + cH + cL_p \sin \rho_{PE} = R_p \cos(\rho_{AE} + \phi) \quad (20)$$

Substituting $L_p = H/\cos \rho_{PE}$, $W_p = \frac{1}{2}\gamma H^2 \cot \rho_{PE}$, $Q = qH \cot \rho_{PE}$, $S_Q = f k_h Q$ and rearranging,

$$P_{PE} = \frac{\cos(\rho_{PE} + \phi)}{\cos(\rho_{PE} + \phi + \delta)} [\tan(\rho_{PE} + \phi) - k_h] \left[2 \frac{q}{H} + \gamma \right] \frac{H^2}{2} + \frac{\cos(\rho_{PE} + \phi)}{\cos(\rho_{PE} + \phi + \delta)} \left[2 \tan(\rho_{PE} + \phi) + \frac{1}{\tan \rho_{PE}} \right] cH \quad (21)$$

Since P_{PE} involves more than one variable, it is impossible to obtain a direct expression like Equation (12). However, setting $c'' = c/\gamma H$ and $q'' = q/\gamma H$, the minimum P_{PE} can be obtained for any given q and c as

$$P_{PE} = A_1' (2q'' + 1) \frac{1}{2} + A_2' c'' \quad (22)$$

where

$$A_1' = \frac{\cos(\rho_{PE} + \phi)}{\cos(\rho_{PE} + \phi + \delta)} [\tan(\rho_{PE} + \phi) - k_h] \quad (23)$$

$$A_2' = \frac{\cos(\rho_{PE} + \phi)}{\cos(\rho_{PE} + \phi + \delta)} \left[2 \tan(\rho_{AE} + \phi) + \frac{1}{\tan \rho_{AE}} \right] \quad (24)$$

Equilibrium of the active wedge leads to the expression for the active seismic thrust:

$$P_{AE} = \left[\frac{2p_{LE} + \gamma}{H} \right] A_1 \frac{H^2}{2} + \left[\frac{2p_{LE} f k_h + \gamma}{H} \right] A_2 \frac{H^2}{2} - A_3 cH \quad (25)$$

where

$$A_3 = \frac{\cos(\rho_{PE} - \phi)}{\cos(\rho_{AE} - \phi - \delta)} \left[2 \tan(\rho_{AE} - \phi) + \frac{1}{\tan \rho_{AE}} \right]$$

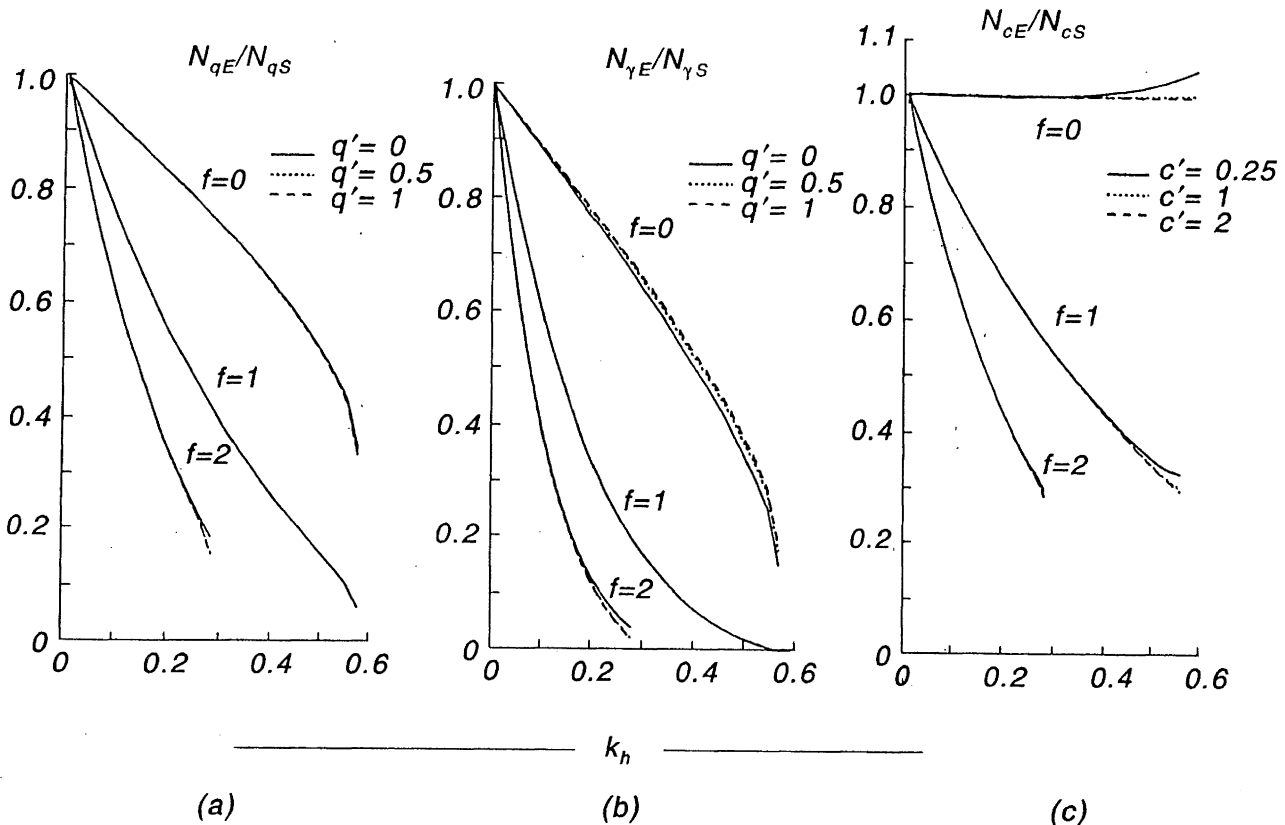


FIGURE 8 Comparison of the ratio of seismic to static coefficients for $\phi = 30^\circ$ (Coulomb)

and A_1 and A_2 are given by equations (10) and (11). If $p''_{LE} = p_{LE}/\gamma H$,

$$P'_{AE} = (2p''_{LE} + 1)A_1 \frac{1}{2} + (2p''_{LE}fk_h + 1)A_2 \frac{1}{2} - A_3c'' \quad (26)$$

Again the total active force must equal the total passive force. Iterating, P_{AE} and p_{LE} are determined at some ρ_{AE} . Here, as in the solution by the method of characteristics, N_{qE} and $N_{\gamma E}$ are fixed by equations (17) and (18) and N_{cE} is calculated by superposition. Thus,

$$N_{cE} = \frac{A_3 + A_2'}{A_1 + fA_2} \quad (27)$$

The ratio of N_{cE} to N_{cS} is shown in Figure 8c with varied c'' where N_{cS} is 30.94, 30.89 and 30.88 for $c'' = 0.25, 1$ and 2 , respectively. As before, the variations of c'' has little effect for $\phi = 30^\circ$ or, for that matter, for other ϕ values between 10° and 40° .

COMPARISON FOR DESIGN

Two methods to determine seismic bearing capacity have been presented. The method of characteristics is rigorous and is considered the most sophisticated approach for limit analysis even though it solves for a nonuniform bearing pressure and base shear distribution. On the other hand the upper bound equilibrium method using the Coulomb mechanism with $\delta = \phi/2$ is only approximate but it solves for the loading prescribed and is simple to use. Comparison of the ratio of the seismic to static coefficients plotted in Figure 9 shows that the results are very close to each other. Figure 10a and 10b show the similarity in the slip surfaces predicted by each method for the static case and for $f = 1.0, k_h = 0.4$. To compare the results obtained by Sarma and Iossifelis [1990], which are only for $f=1$, the case for $\phi=30^\circ$ is shown in Figure 11 (the values of Sarma's method are scaled from their paper). Thus the results by all methods are extremely close to one another.

One interesting result by both methods presented in this paper is that the ratios of seismic to static coefficients are insensitive to changes in the parameters q' and c' . For design, this allows a single set of curves to be drawn based on the parameters f and ϕ . Families of curves including q and c are unnecessary.

From the results it seems that the simple and straightforward method resulting from the Coulomb mechanism can replace the much more complicated method of characteristics. Thus, the use of the values calculated by the Coulomb mechanism is recommended for design and Figure 12 is presented to give a complete set of bearing capacity ratios for that purpose. These curves are a refined version of those presented by Richards et al. [1993] improved to include a nonempirical solution for N_{cE} and the variable shear transfer.

With these curves the sliding block analysis can be used as shown in Figure 13 to calculate seismic settlements with the geometric relationship shown in Figure 14:

$$w = 2\Delta \tan \rho_{AE} \quad (28)$$

wherein Δ is the horizontal sliding block displacement of the fictitious wall dividing the active and passive wedges and ρ_{AE} is the active wedge angle.

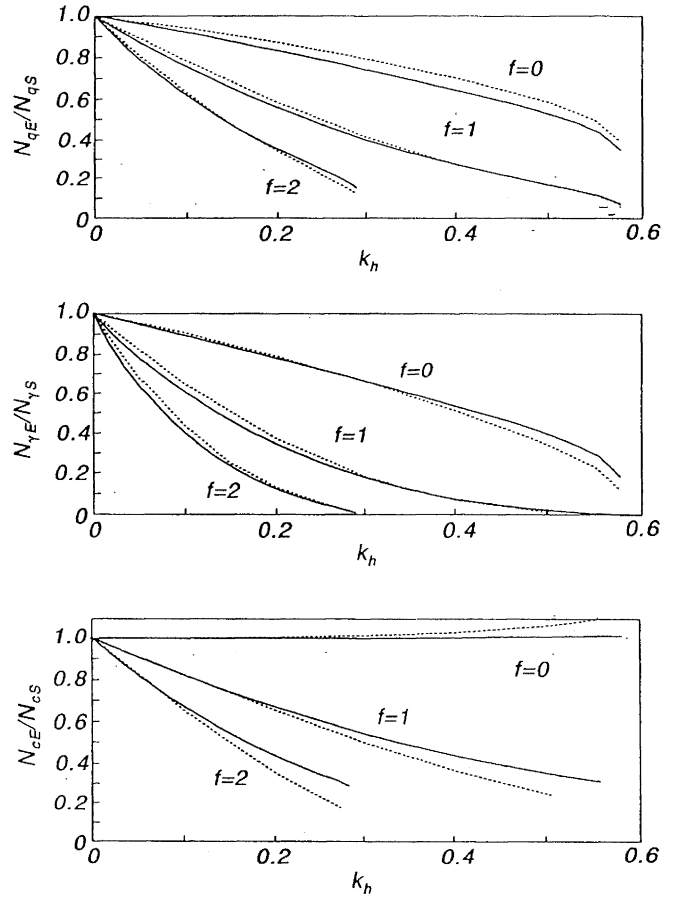


FIGURE 9 Comparison between the Coulomb mechanism method (solid) and the method of characteristics (dotted)

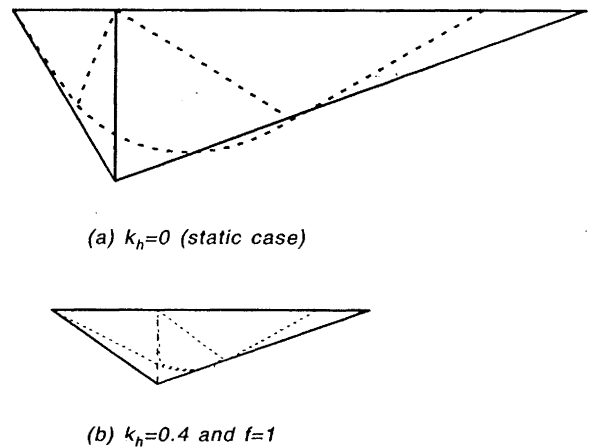


FIGURE 10 Comparison of the slip surfaces between "Coulomb" (solid line) and "Characteristics" (dotted line); $\phi = 30^\circ, c = 1, q' = 0.5$

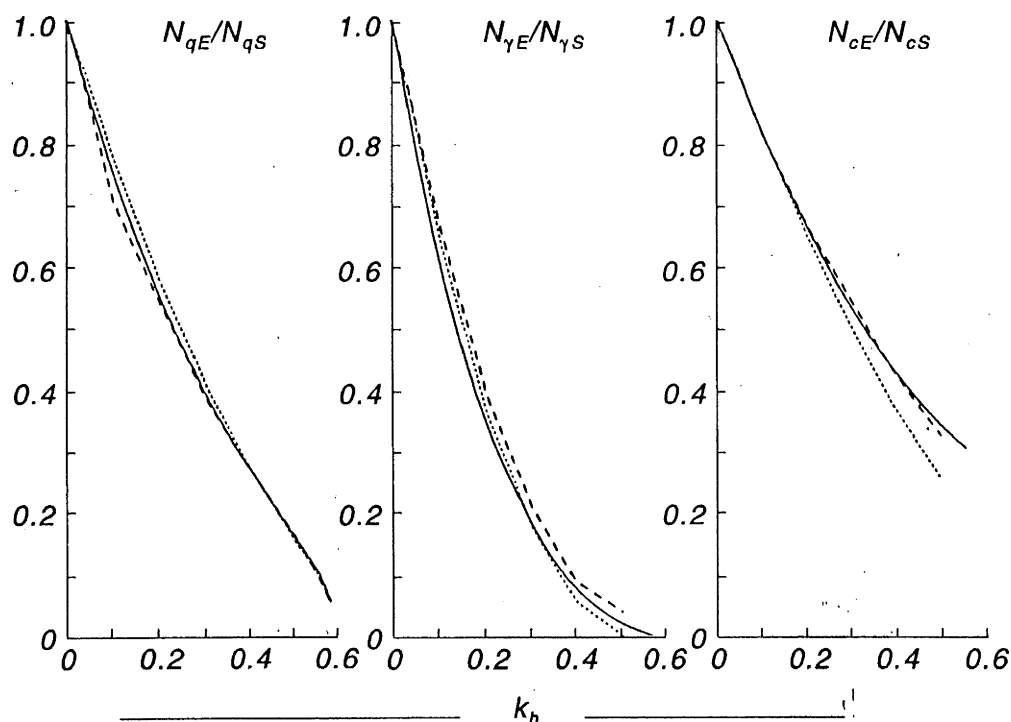


FIGURE 11 Comparison among "Coulomb", "Characteristics" and "Sarma" for $\phi = 30^\circ$, $f = 1$

The sliding block displacements have been calculated for a number of standardized earthquake records by Newmark [1965], Franklin and Chang [1977] and others, leading to various approximate expressions for displacements. The straight-line relation suggested by Richards and Elms [1979] is appropriate for displacements of retaining walls:

$$\Delta = 0.087 \frac{V^2}{Ag} \left[\frac{k_h^*}{A} \right]^{-4} \quad (29)$$

where V and A are the maximum velocity and acceleration coefficients of the design earthquake and g is the gravitational acceleration, all in consistent units. The cut-off or critical acceleration, k_h^* , depends, of course, on the design. Here, it should also be pointed out that the change in the active wedge angle, ρ_{AE} , with q and c as shown in Figure 14 is not significant. Thus, one set of curves for ρ_{AE} for various f as shown in Figure 15 is sufficient for design.

As an example of the procedure to determine the seismic settlement of an existing footing, consider a surface footing on granular soil ($c=0$) with $\phi = 30^\circ$, $\gamma = 17.3 \text{ KN/m}^2$ (110 lb/ft³) and $B = 1.2 \text{ m}$ (4 ft) for an earthquake of intensity $A = 0.3$, $V = 0.38 \text{ m/sec}$ (15 in/sec) which has a static factor of safety of 3. To determine the critical acceleration, Figure 12c can be used directly or it can be replaced by the curves for Static Factors of Safety vs. acceleration coefficient shown in Figure 16. Therefore, if $f = 0$, then $k_h^* = 0.23$, $\tan \rho_{AE} = 0.96$ and therefore $w = 23 \text{ mm}$ (0.9 in). For $f = 2$, $k_h^* = 0.12$, $\tan \rho_{AE} = 0.9$ and $w = 302 \text{ mm}$ (11.9 in).

As a second example, assume a footing on soil with $c = 9.6 \text{ KN/m}^2$ (200 lb/ft²), $\phi = 30^\circ$ with $d/B = 0.25$ and the other parameters the same as for the first example. For this general

case, Figure 13 must be used with trial and error to determine the k_h^* . The static coefficients are $N_{qS} = 16.5$, $N_{cS} = 30.9$ and $N_{\gamma S} = 23.8$ and therefore $p_{LS} = 193 \text{ KN/m}$ (13230 lb/ft). For $f = 0$, there is obviously no settlement since the soil is stronger than in the first example. With $f = 1$, $k_h^* = 0.34$, and again there will be no settlement. For $f = 2$ however, $k_h^* = 0.19$, $\tan \rho_{AE} = 0.65$ and the footing will settle $w = 35 \text{ mm}$ (1.4 in).

From a design perspective, most structures can sustain some settlement and the procedure can be reversed to determine the static factor of safety to limit the seismic settlement to some allowable value. For example, if the allowable maximum settlement is 25 mm for a footing with $B = 18.3 \text{ m}$ (60 ft), $d/B = 0.15$ and the other parameters γ , ϕ , c , A and V are the same as in the second example, $p_{LS} = 1475 \text{ kN/m}$ for $f = 1$. Assume $\tan \rho_{AE} = 0.95$, then $k_h^* = 0.23$ from equation (29) and, from Figure 16, $\tan \rho_{AE} = 0.96$ which is sufficiently close and no iteration is necessary. From Figure 13 with this value of k_h^* , the ratio of seismic to static coefficients are obtained as: $N_{cE}/N_{cS} = 0.60$, $N_{qE}/N_{qS} = 0.49$, and $N_{\gamma E}/N_{\gamma S} = 0.28$. Therefore, the required static F.S. for the footing is determined as 3 for this earthquake. On the other hand if the allowable settlement were only 12 mm (0.5 in) the required static F.S. would be 3.6.

CONCLUSIONS

The solution for seismic bearing capacity factors for a simple Coulomb mechanism based on limit force equilibrium of two wedges with assumed friction between them of $\delta = \phi/2$ is verified as satisfactory by comparison to the solution by the method of characteristics. The results show that for drained soils only the shear transfer, f , at the base of the footing and the

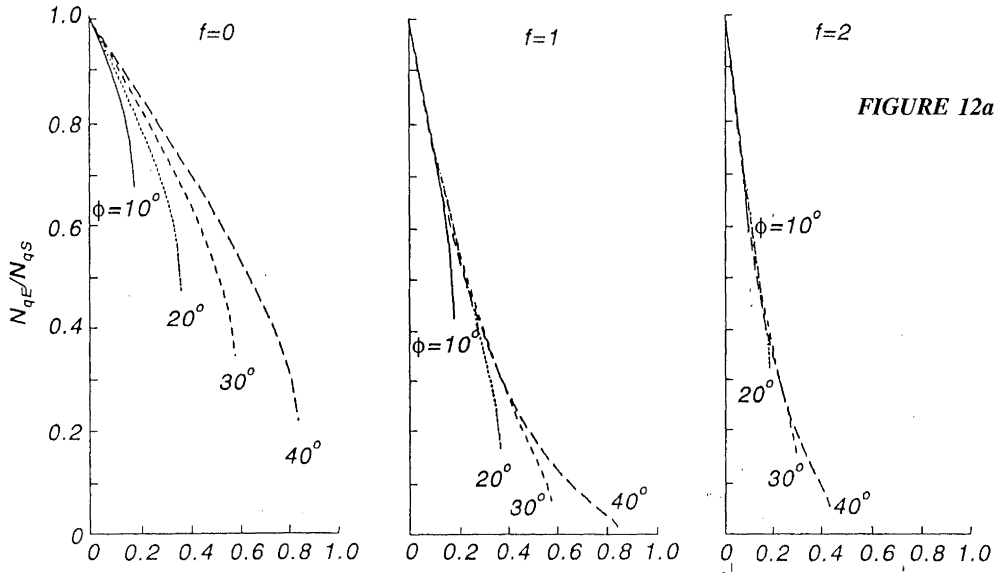


FIGURE 12a Ratio of N_{qE} to N_{qs} for design

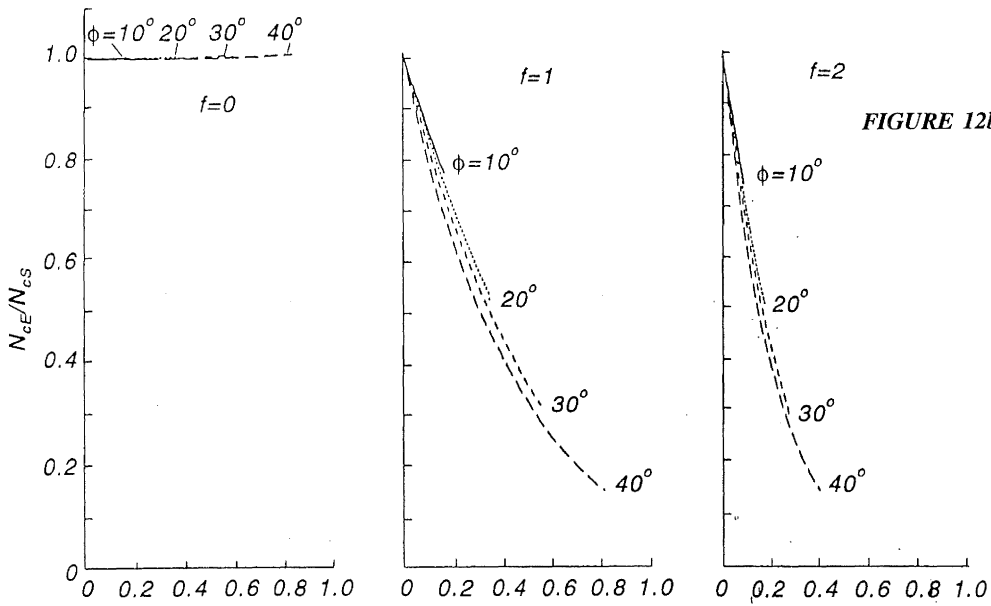


FIGURE 12b Ratio of N_{cE} to N_{cs} for design

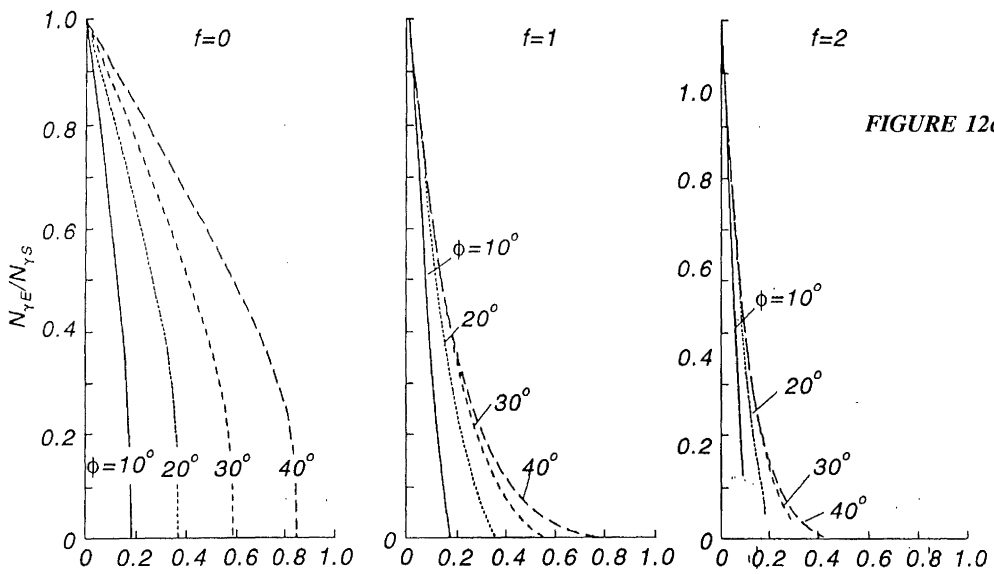


FIGURE 12c Ratio of $N_{\gamma E}$ to $N_{\gamma S}$ for design

k_h

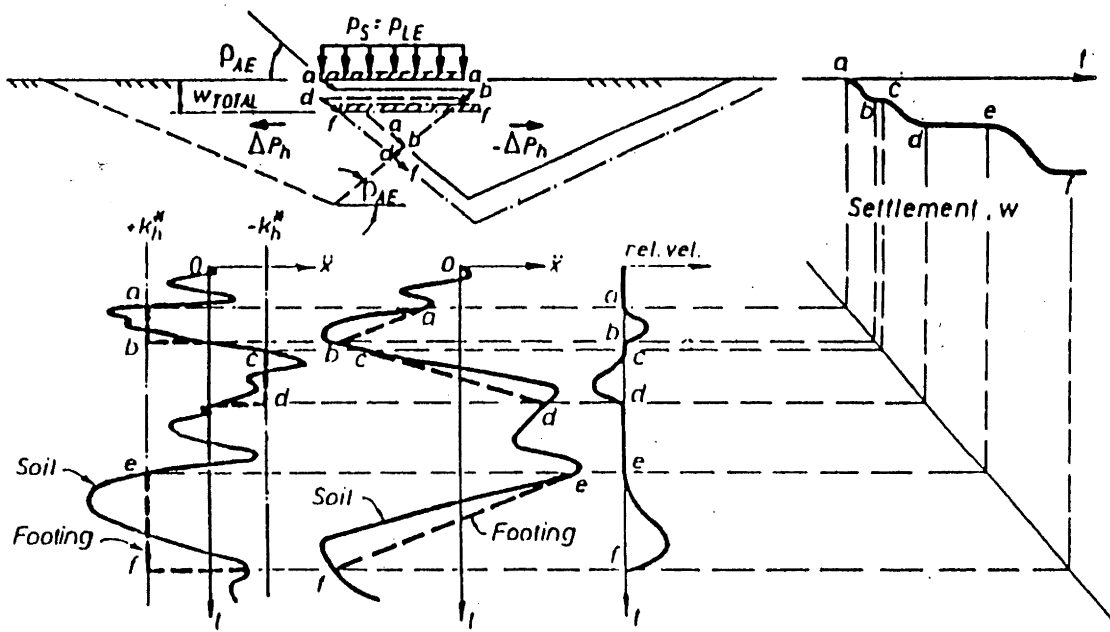


FIGURE 13 The sliding block method to calculate seismic settlement

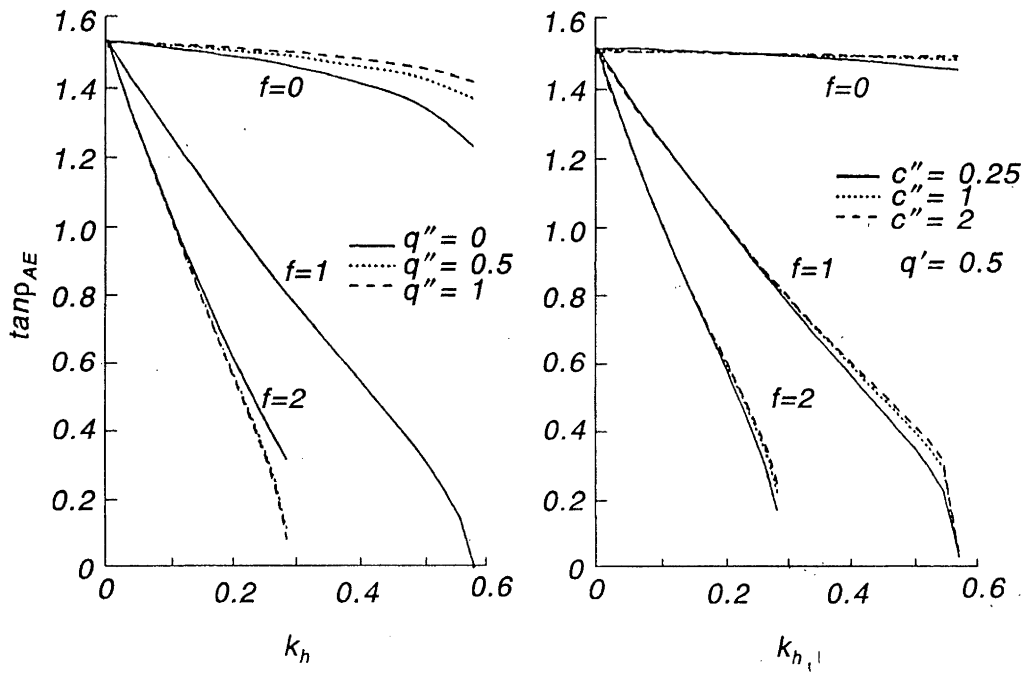


FIGURE 14 Comparison of $\tan \rho_{AE}$ for $\phi = 30^\circ$

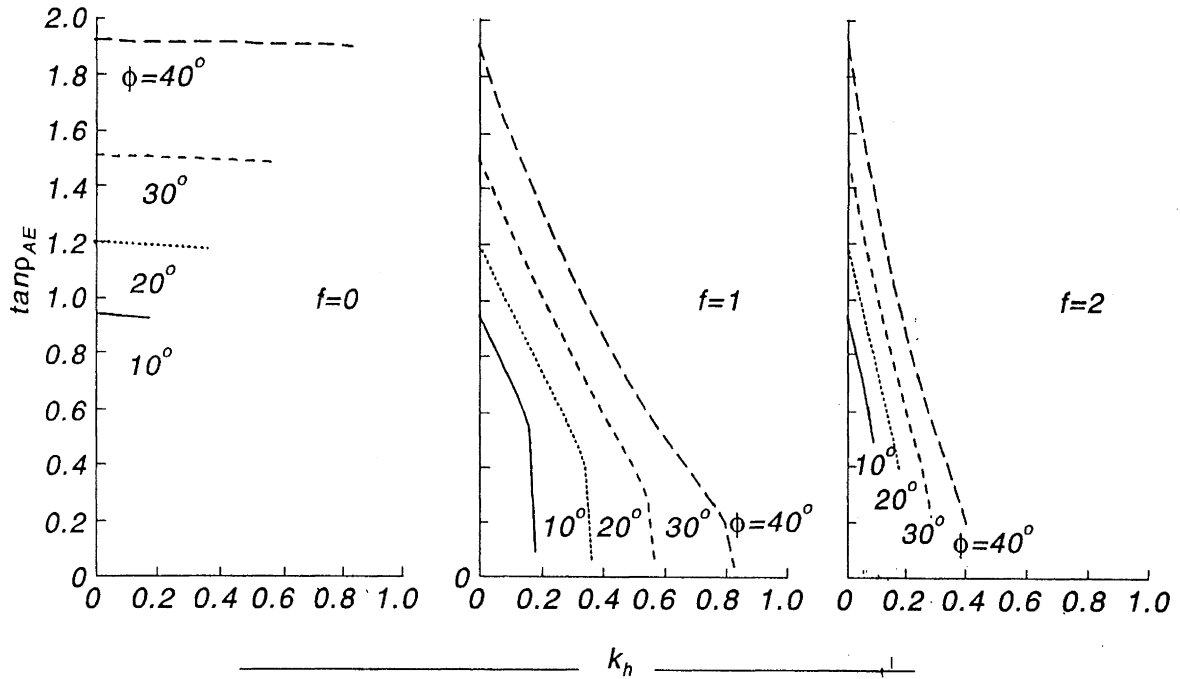


FIGURE 15 $\tan \rho_{AE}$ for design

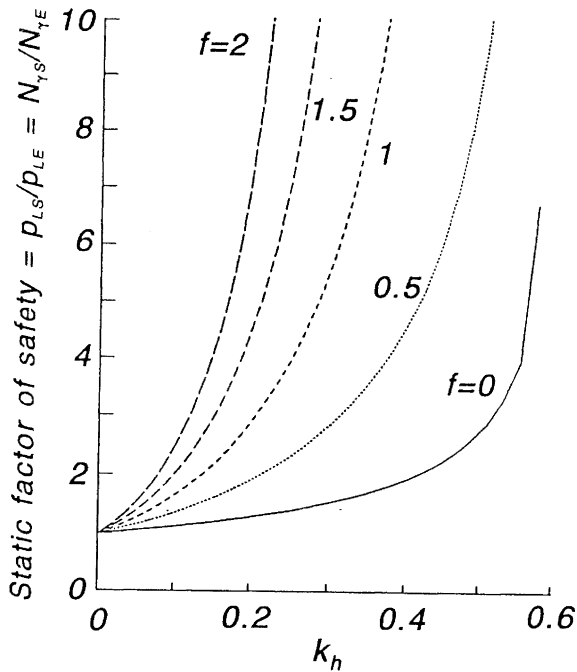


FIGURE 16 Static factor of safety for surface footing with $\phi = 30^\circ$ and $c = 0$

inertial shear stress in the soil built up by the earthquake acceleration are significant in the seismic degradation of bearing capacity. Their individual effects can be seen in Figure 12. The loss in bearing capacity due only to the build up of inertial forces in the soil mass is the case $f = 0$. This can be subtracted from the total loss for $f > 0$ to determine the separate effect of the shear transfer at the base of the footing.

The insensitivity of the solution for the bearing capacity factors to q and c allows the development of design curves for the ratio of seismic to static coefficients. Such design variables as the shape of the footing are therefore included directly in the value for the static bearing capacity factors. As an alternative, the total seismic bearing capacity can be calculated directly from the equations. For cohesionless soils the design curves presented to calculate the seismic bearing capacity and settlements are complete while for cohesive soils, beyond the acceleration inducing general fluidization, the total seismic bearing capacity must be calculated.

The most serious case in practice may be structures such as tanks or buildings on matt footings where $f = 1$. Codes now call for static factors of safety of from 2 to 3. Such structures, as shown in the example, will begin to settle incrementally at an acceleration $k_h^* = 0.23$, which is not uncommon in a moderate earthquake. The same would be true for strip and isolated footings with static factors of safety in this range. Footings for bridge piers usually have a higher static factor of safety because of live load factors and impact provisions in the code. However, even here, a moderate earthquake may cause problems if the girder design is indeterminate limiting allowable settlements while increasing the shear transfer coefficient f .

ACKNOWLEDGEMENT

This work was supported in part by a research grant from the National Center for Earthquake Engineering Research at SUNY/Buffalo on the seismic behaviour of bridge foundations. It is an outgrowth of previous work on tied-back walls supported by NSF and the New Zealand Roads Board.

REFERENCES

- Budhu, M. and Al-Karni. 1993. Seismic Bearing Capacity of Soils, *Geotechnique*, 43(1):181-187.
- Franklin, A.G. and F.K. Chang. 1977. *Earthquake Resistance of Earth and Rock-Fill Dams: Report 5: Permanent Displacements of Earth Embankments by Newmark Sliding Block Analysis*, Miscellaneous Paper S-71-17, Soils and Pavements Laboratory, U.S. Army Engineer Waterways Experiment Station, Vicksburg, Miss., Nov.,
- Harr, M.E. 1966. *Foundations of Theoretical Soil Mechanics*, McGraw Hill Inc., New York.
- Newmark, N.M. 1965. Effects of Earthquakes on Dams and Embankments, *Geotechnique*, 15(2):139-160.
- Richards, R., D.G. Elms, and M. Budhu. 1993. Seismic Bearing Capacity and Settlements of Foundations, *Journal of Geotechnical Engineering*, ASCE, 119(4):662-674.
- Richards, R. and X. Shi. 1991. Seismic Bearing Capacity of Shallow Foundations, *Proc. Pacific Conf. on Earthquake Engineering*, November 20-23, Auckland, New Zealand.
- Richards, R., D.G. Elms, and M. Budhu. 1990a. Dynamic Fluidization of Soils, *Journal of Geotechnical Engineering*, ASCE, 116(5):740-759.
- Richards, R., D.G. Elms, and M. Budhu. 1990b. Soil Fluidization and Foundation Behaviour, *Proc. 2nd Int. Conf. Recent Advances in Geotechnical Earthquake Engineering and Soil Dynamics*, Rolla, MO, 1:719-723.
- Richards, R. and D.G. Elms. 1987. *Seismic Behaviour of Tied Back Walls*, Report 87-8, Dept of Civil Engineering, University of Canterbury, Christchurch, NZ.
- Richards, R. and D.G. Elms. 1979. Seismic Behaviour of Gravity Retaining Walls, *Journal of Geotechnical Engineering*, ASCE, 105(GT4):449-464.
- Sarma, S.K. and I.S. Iossifelis. 1990. Seismic Bearing Capacity of Shallow Strip Footings, *Geotechnique*, 40(2):265-273.
- Shi, X. 1993. *Plastic Analysis for Seismic Stress Fields*, Dissertation, Dept of Civil Engineering, SUNY at Buffalo.
- Sokolovsky, V.V. 1960. *Statics of Soil Media*, Translated by Jones, D.H. and Schofield, A.N., Butterworths, London.